On the Positive Effect of CO during Start/Stop in High-Temperature Polymer Electrolyte Fuel Cells

On the Positive Effect of CO during Start/Stop in High-Temperature Polymer Electrolyte Fuel Cells

Tom Engl, Jörn Käse, Lorenz Gubler,* and Thomas J. Schmidt*,z

Electrochemistry Laboratory, Paul Scherrer Institut, 5232 Villigen PSI, Switzerland

The influence of CO in the fuel gas on cathode carbon corrosion during start/stop cycles in high temperature polymer electrolyte fuel cells (HT-PEFC) was investigated. The fuel cell underwent simulated start/stop cycles with a constant time interval, reactant gas flow rate and temperature by switching between H_2/CO mixtures and O_2 at the fuel electrode. The results reveal that increasing amounts of CO in the fuel gas reduce the amount of carbon corrosion at the air electrode. Therefore, HT-PEFC operation with CO containing fuel has the benefit of mitigating start/stop induced degradation effects.
 [DOI: 10.1149/2.0011407eel]

Manuscript submitted March 10, 2014; revised manuscript received April 11, 2014. Published May 1, 2014.

One of the most beneficial and unique features of a high-temperature polymer electrolyte fuel cell (HT-PEFC) is the capability to tolerate orders of magnitude lager amounts of CO (up to 3%)[1,2] compared to a LT-PEFC (approx. 10 ppm).[3] Therefore, the system can be used to generate electricity from hydrogen-rich reformate gases without complex and energy intensive CO-cleanup.

Nevertheless, the HT-PEFC can suffer from numerous degradation effects in different locations of the membrane electrode assembly (MEA),[4] e.g. pinhole formation in the membrane, acid evaporation and membrane thinning.[5,6] Electrodes can also represent a major area of degradation. Interestingly, specific degradation mechanisms, such as carbon corrosion, catalyst detachment and catalyst particle growth (Ostwald-ripening) can be found in the LT-PEFC as well. Additionally, structural changes and acid flooding of the porous layers of the cell can occur. All degradation mechanisms are complex functions of the specific operation conditions, making their individual identification challenging. Hence, it is necessary to gain insight into limitations of MEA lifetime, which is the key to successful development of mitigation strategies to reach the desired lifetimes, i.e. >40.000 hours[6] for stationary applications.

One of the specific degradation triggers is known as "reverse-current decay" or "start/stop"- mechanism, respectively.[7–9] This degradation mode is induced during fuel cell start-up or shut-down, when air or pure oxygen and fuel gas co-exist in the fuel electrode compartment (see Figure S1 and its description in the supplemental material). This mechanism can be one of the main reasons for carbon corrosion at the air electrode. The number of start/stop cycles is closely related to the overall lifetime of the fuel cell if the induced degradation effects are not mitigated. If, for instance, a HT-PEFC is used in a combined heat and power (CHP)[10–12] system, it is conceivable that several hundred cycles will be accumulated, which can lead to a rapid and irreversible damage of the stack.[13] It is necessary, therefore, to improve the understanding of the start/stop mechanism in order to deduce appropriate mitigation strategies. Mitigation strategies can be divided into two categories. One is focused on developing new materials, such as carbon free electrodes[14–16] or selective hydrogen oxidation catalysts.[17–19] The second category consists of system strategies, for instance flow rate adjustements,[20,21] cell potential control[8] or nitrogen purging.[8,22] Therefore, this investigation is categorized as system based fuel cell degradation mitigation strategy.

Experimental

All experiments were carried out with BASF Celtec membrane electrode assemblies. Those MEAs consist of a H_3PO_4 doped PBI membrane[4] and carbon paper based gas diffusion electrodes (Pt/Vulcan XC-72, 1 $mg_{Pt}cm^{-2}$ on the fuel and air electrode, respectively). The MEA thickness is approximately 820 µm including a membrane thickness of around 50–75 µm. The cells (active area 45.15 cm^2) were operated at ambient pressure and were supplied with dry process gases with stoichiometries of 1.2 for hydrogen and 2.0 for air during break-in. Simulated start/stop experiments were carried out by switching the gas fed to the fuel electrode between different CO/H_2 mixtures (as model gas simulating reformate) and O_2. The experiments were carried out in three different phases. During the first phase 90 vol% H_2 (with 10 vol% N_2) and O_2 were used as alternating supply gases on the fuel electrode (no CO present). The first phase is necessary in order to condition the electrode and to create a reference for phase 2. A reference is needed for calculating the amount of mitigated carbon corrosion corresponding to one specific CO partial pressure (p_{CO}). During the second phase the H_2/CO ratio was gradually varied. The H_2 partial pressure was maintained constant at 90 vol% whereas p_{CO} was increased from 0 vol% in steps of 1 vol% up to 10 vol% with N_2 as balance (Figure 1). Note that 9 vol% CO could not be set due to flow controller limitations. Whereas during the second phase the CO partial pressure was increased from 0 to 10 vol%, during the third phase the CO content was decreased from 10 to 0 vol%. Thereby, potential hysteresis effects can be identified. Before the third phase was started two start/stop cycles were measured without CO in order to create a reference for the last phase. The reference for the second phase is deduced from the last two start/stop cycles of the first phase. A cycle time of 180 seconds was chosen for switching between the simulated reformate and oxygen on the fuel electrode side, allowing fuel/O_2 (O_2/fuel) fronts to pass through the fuel electrode simulating start-up and shut-down processes (complete simulated start/stop cycle in 360 s). The air electrode was constantly fed with pure oxygen during the start/stop experiments. The denotation of the electrodes follows the proposition in reference:[23] the electrode normally operated as fuel cell anode is named fuel electrode, whereas the electrode normally operated as fuel cell cathode is denoted as air electrode.

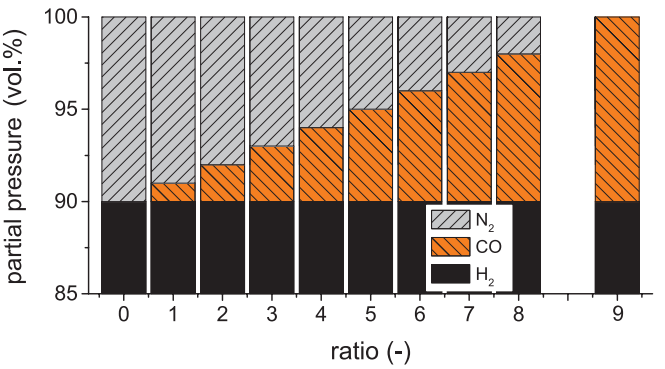

Figure 1. Anode fuel gas composition. Hydrogen is kept constant at 90 vol%, whereas p_{CO} is in/decreased in steps of 1 vol%. N_2 is used as buffer.

*Electrochemical Society Active Member.
zE-mail: thomasjustus.schmidt@psi.ch

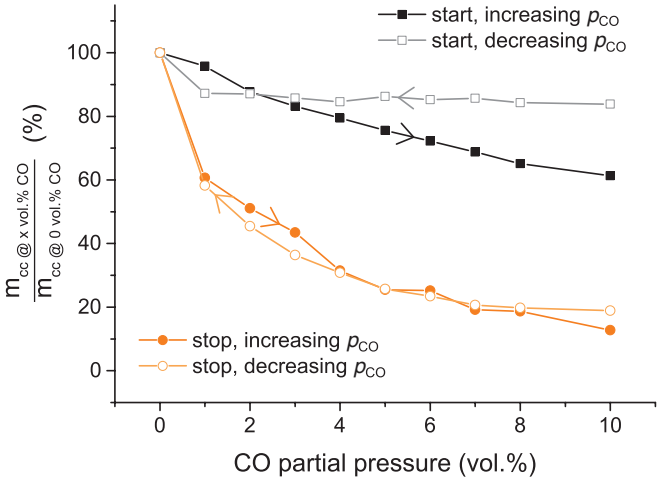

Figure 2. Change of corroded carbon on the air electrode corresponding to a given CO partial pressure on the fuel electrode. The solid symbols represent the measurements with increasing p_{CO} whereas the open symbols indicate the measurements with decreasing p_{CO}. Measuring conditions: 180°C, fuel electrode with varying supply gas composition @ 40 $L_n h^{-1}$, cathode with O_2 @ 40 $L_n h^{-1}$.

The fuel and air electrode flow rate was set to 40 $L_n h^{-1}$ resulting in a residence time of the fuel/O_2 (O_2/fuel) fronts of 0.39 s. The cell temperature was held at 180°C. The carbon corrosion was measured via the CO_2 signal in the air electrode exhaust gas using a real time infrared CO_2 detector with a detection range up to 10'000 ppm_{CO2} (California Analytical Instruments Model 601). For each mixing ratio two consecutive start and stop events were recorded. The mass of corroded carbon m_{cc} was calculated by averaging two start and stop CO_2 peaks, respectively, at a given CO partial pressure:

$$m_{cc} = M_C \cdot n_{CO_2} = M_C \frac{p\dot{V}}{RT} \cdot A_{CO_2-peak} \quad [1]$$

where A_{CO_2-peak} is the area of the CO_2 peak (ppms), p and T are the ambient pressure and temperature, respectively, R is the universal gas constant, M_C is the molar mass of carbon, and $\dot{V}$ is the effective volumetric gas flow rate. In Figure 2 the relative decrease of corroded carbon is illustrated as the ratio of the mass of corroded carbon at a given CO partial pressure ($m_{cc\ @\ x\ vol\%\ CO}$) to the mass of corroded carbon at 0 vol% CO ($m_{cc\ @\ 0\ vol\%\ CO}$). Two three-way magnetic valves (Bürkert Type 0330) are used for switching the fuel electrode gas supply intermittently.

Results and Discussion

A series of simulated start/stop procedures was performed with varying CO partial pressures in the fuel gas. The measured CO_2 signals are higher for start than for stop events, which is usually ascribed to pseudo-capacitive electrode reactions upon the potential changes during the start/stop processes ('pseudo-capacitive' effect)[7,13,24–26] (we refer to Figure S2 for the original CO_2 signals). More importantly, the measurements indicate that an increasing CO partial pressure in the model reformate leads to a decrease of the CO_2 amount released in the air electrode during the simulated start/stop cycles.

The trend of corroded carbon during start/stop cycles at different CO partial pressures is illustrated in Figure 2. Increasing the CO concentration on the fuel electrode leads to a decrease of CO_2 formation on the air electrode, pointing to a reduced amount of corroded carbon. For start events the mitigation effect is less pronounced than for stop events. Furthermore, within our experimental conditions the results indicate that for stop events the order of changes in the CO partial pressure (increasing or decreasing) is not relevant. The mitigation effect remains nearly the same. In contrast, for start events the order of the experimental change of CO content appears to be more beneficial if the partial pressure is increased (0 vol% to 10 vol%) rather than decreased (10 vol% to 0 vol%). Further studies are underway to better understand this effect and will be reported elsewhere.

The gradually declining carbon corrosion with increasing CO content in the fuel electrode gas can be explained conclusively with the sketch in Figure 3. In order to oxidize carbon on the air electrode in the passive fuel cell section (=load) hydrogen needs to be oxidized on the fuel electrode in the active fuel cell section (=source, see Figure S1 and references).[7,8] If the CO partial pressure increases, the available number of free sites on the fuel electrode catalyst for the hydrogen oxidation reaction is diminished (Figure 3a vs. Figure 3b) due to high CO coverages. Therefore, less hydrogen is oxidized, which consequently leads to a smaller amount of oxidized carbon due to the conservation of the charge and current balances, which is in agreement with the observed increasing anode overpotential during fuel cell operation with CO-containing hydrogen as shown in Ref. 27. Higher anode overpotentials lead to reduced HOR and ORR currents on the fuel electrode and, as a consequence, to smaller carbon corrosion currents (less corroded carbon) on the air electrode. Increasing the CO coverage on the fuel electrode catalyst surface causes a effect similar than reducing the Pt loading on the same electrode, as discussed previously.[24]

The proposed model is furthermore able to explain the different amounts of produced CO_2 for start and stop events at various CO partial pressures. In the stopped cell, no or only a negligible number of surface sites are covered by CO (only oxygen is present in the fuel electrode). Introducing CO/H_2 into the fuel electrode upon start-up (at 180°C in our experiments), CO adsorption on the catalyst surface competes with the very fast hydrogen oxidation kinetics, i.e., only a limited number of sites will be covered by CO (Figure 4a) and the overall corrosion current is determined by the hydrogen oxidation reaction on a surface slightly covered by CO.

A contrary behavior can be observed during stop events (Figure 4b). The entire fuel electrode catalyst surface is, depending on the CO partial pressure, covered by CO at its equilibrium saturation coverage. If now the fuel cell is stopped oxygen is introduced to the fuel electrode and the corrosion current is determined by the hydrogen oxidation on a Pt surface with CO saturation coverage, which is significantly lower as compared to the start process when the CO coverage is low.

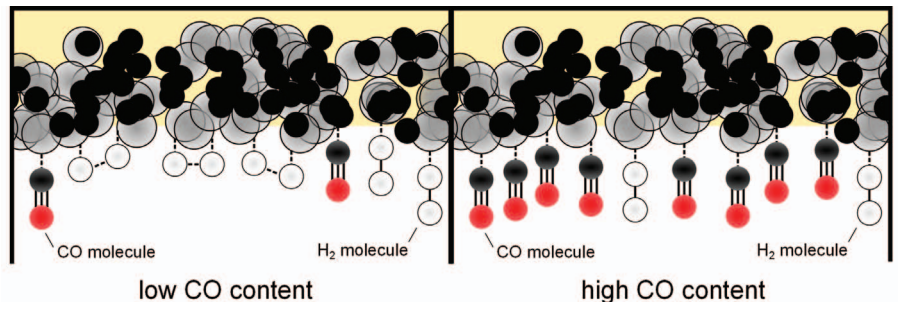

Figure 3. Anode catalyst surface sketches with low and high CO partial pressures in the reformate gas resulting in low and high CO equilibrium coverages on the fuel electrode catalyst surface.

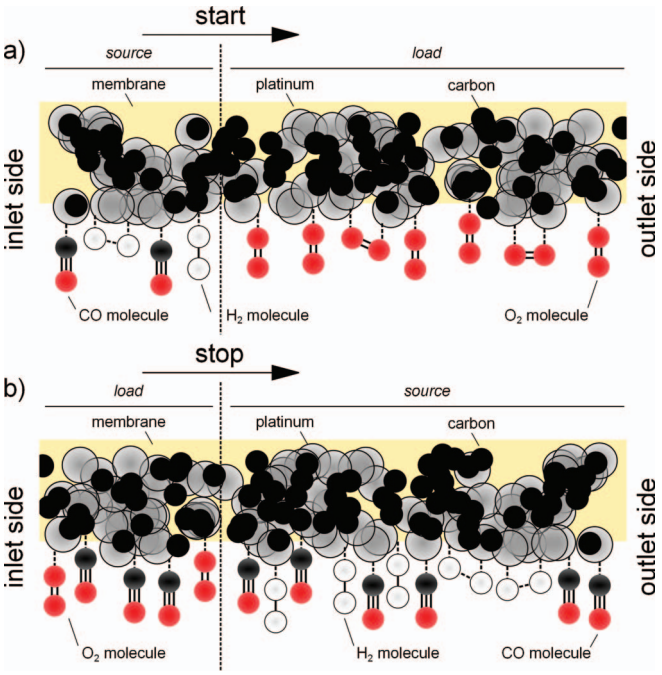

Figure 4. Sketch of the fuel electrode processes during a start a) and stop b) transient with CO in the reformate gas.

Additionally, during the introduction of oxygen onto a CO covered Pt surface, an air-bleed effect may be observed, i.e., the chemical oxidation of CO by O_2 reduces the number of electrochemical oxygen reduction turnovers due to surface near O_2 partial pressure reduction.

Since during the passage of a fuel/O_2 (O_2/fuel front) the reverse current in the load (O_2/O_2) section of the cell must be equal to the source section (fuel/O_2; for details see also the discussion of the intercept of the individual source and load polarization curves in Ref. 23), in a start event only the fuel/O_2 section is affected by the presence of CO, whereas in the stop event, both sections (i.e., the complete cell) is affected by CO, leading to an overall lower corrosion current.

Conclusions

The HT-PEFC can be operated with a rather high content of CO[1,2] of several percent in the reformate fuel. Here, it is shown that the presence of CO in the fuel gas can mitigate start/stop induced carbon corrosion at the cathode. Increasing the CO content on the fuel electrode side during start/stop results in a reduced CO_2 formation on the air electrode side indicating a reduced amount of oxidized carbon. Compared to pure H_2 without CO, a partial pressure of 10 vol% CO in the reformate gas (typical CO volume fraction at a reformer exhaust)[28] reduces the amount of corroded carbon between 16 and 39% for start and between 81 and 87% for stop events. Therefore, it is not only possible but desirable to use CO containing fuel gases to improve the overall lifetime of the fuel cell. Conceptually, this positive effect of the presence of CO on the corrosion during start/stop processes might be even more pronounced in LT-PEFC due to very fast CO adsorption kinetics on Pt and significantly higher CO saturation coverages.[27,29–32]

Acknowledgments

Financial support from BASF SE is gratefully acknowledged. We thank Christian Marmy and André Meier for technical assistance and our colleges at the PSI for productive discussions.

References

1. T. J. Schmidt and J. Baurmeister, *ECS Trans.*, **3**, 861 (2006).
2. Q. Li, R. He, J. O. Jensen, and N. J. Bjerrum, *Fuel Cells*, **4**, 147 (2004).
3. A. D. Modestov, M. R. Tarasevich, V. Y. Filimonov, and E. S. Davydova, *Electrochim. Acta*, **55**, 6073 (2010).
4. T. J. Schmidt, *High-Temperature Polymer Electrolyte Fuel Cells: Durability Insights* F. N. Büchi, M. Inaba, and T. J. Schmidt, Editors, p. 199–221 Springer New York, New York, NY (2009).
5. A. D. Modestov, M. R. Tarasevich, V. Y. Filimonov, and N. M. Zagudaeva, *Electrochim. Acta*, **54**, 7121 (2009).
6. T. J. Schmidt, *ECS Trans.*, **1**, 19 (2006).
7. W. Gu, R. N. Carter, P. T. Yu, and H. A. Gasteiger, *ECS Trans.*, **11**, 963 (2007).
8. C. A. Reiser, L. Bregoli, T. W. Patterson, J. S. Yi, J. D. Yang, M. L. Perry, and T. D. Jarvi, *Electrochem. Solid-State Lett.*, **8**, A273 (2005).
9. P. T. Yu, W. Gu, R. Makharia, F. T. Wagner, and H. A. Gasteiger, *ECS Trans.*, **3**, 797 (2006).
10. G. Giacoppo, O. Barbera, A. Carbone, I. Gatto, A. Saccà, R. Pedicini, and E. Passalacqua, *Int. J. Hydrogen Energy*, **38**, 11619 (2013).
11. P. Moçotéguy, B. Ludwig, J. Scholta, R. Barrera, and S. Ginocchio, *Fuel Cells*, **9**, 325 (2009).
12. P. Moçotéguy, B. Ludwig, J. Scholta, Y. Nedellec, D. J. Jones, and J. Rozière, *Fuel Cells*, **10**, 299 (2010).
13. C. Hartnig and T. J. Schmidt, *J. Power Sources*, **196**, 5564 (2011).
14. A. Rabis, E. Fabbri, A. Foelske, M. Horisberger, R. Kötz, and T. J. Schmidt, *ECS Trans.*, **50**, 9 (2013).
15. S.-Y. Huang, P. Ganesan, and B. N. Popov, *ACS Catal.*, **2**, 825 (2012).
16. J. d'Arbigny, G. Taillades, and J. Rozière, *ECS Trans.*, **41**, 1207 (2011).
17. B. Genorio, D. Strmcnik, R. Subbaraman, D. Tripkovic, G. Karapetrov, V. R. Stamenkovic, S. Pejovnik, and N. M. Marković, *Nat. Mater.*, **9**, 998 (2010).
18. B. Genorio, R. Subbaraman, D. Strmcnik, D. Tripkovic, V. R. Stamenkovic, and N. M. Markovic, *Angew. Chem. Int. Ed. Engl.*, **50**, 5468 (2011).
19. A. Rabis, P. Rodriguez, and T. J. Schmidt, *ACS Catal.*, **2**, 864 (2012).
20. M. L. Perry, T. Patterson, and C. A. Reiser, *ECS Trans.*, **3**, 783 (2006).
21. N. Linse, G. G. Scherer, A. Wokaun, and L. Gubler, *J. Power Sources*, **219**, 240 (2012).
22. J. P. Meyers and R. M. Darling, *J. Electrochem. Soc.*, **153**, A1432 (2006).
23. M. L. Perry, R. M. Darling, S. Kandoi, T. W. Patterson, and C. Reiser, *Stack Durability Operating Requirements for Durable Polymer-Electrolyte Fuel Cell Stacks* F. N. Büchi, M. Inaba, and T. J. Schmidt, Editors, p. 399–417 Springer New York, New York, NY (2009).
24. W. Gu, P. T. Yu, R. N. Carter, R. Makharia, and H. A. Gasteiger, *Modeling ofMembrane-Electrode-Assembly Degradation in Proton-Exchange-Membrane Fuel Cells – Local H2 Starvation and Start–Stop Induced Carbon-Support Corrosion* C.-Y. Wang and U. Pasaogullari, Editors, p. 45–87 Springer New York, New York, NY (2010).
25. S. Kreitmeier, A. Wokaun, and F. N. Büchi, *J. Electrochem. Soc.*, **159**, F787 (2012).
26. A. P. Young, V. Colbow, D. Harvey, E. Rogers, and S. Wessel, *J. Electrochem. Soc.*, **160**, F381 (2013).
27. T. J. Schmidt and J. Baurmeister, *ECS Trans.*, **16**, 263 (2008).
28. A. F. Ghenciu, *Curr. Opin. Solid State Mater. Sci.*, **6**, 389 (2002).
29. T. Engel and G. Ertl, *Adv. Catal.*, **28**, 1 (1979).
30. K. Kunimatsu, T. Sato, H. Uchida, and M. Watanabe, *Langmuir*, **24**, 3590 (2008).
31. H. P. Dhar, L. G. Christner, and A. K. Kush, *J. Electrochem. Soc.*, **134**, 3021 (1987).
32. T. Engl, K. E. Waltar, L. Gubler, and T. J. Schmidt, *J. Electrochem. Soc.*, **161**, F500 (2014).